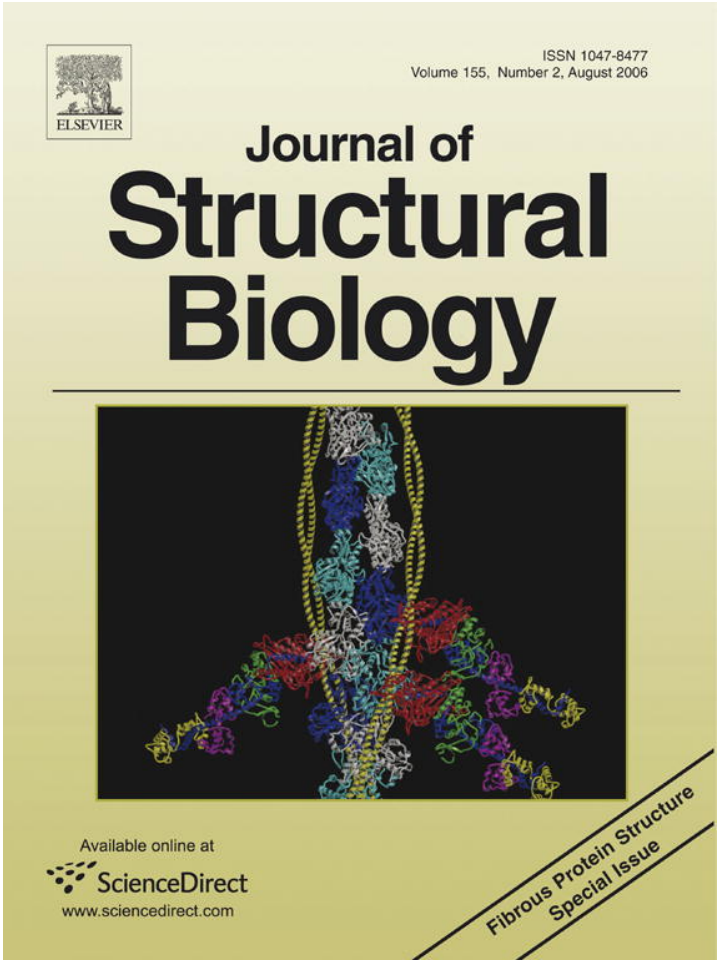

Available online at www.sciencedirect.com
ScienceDirect
Journal of Structural Biology 155 (2006) 263–272
Journal of Structural Biology
www.elsevier.com/locate/yjsbi

Mechanical properties of cardiac titin's N2B-region by single-molecule atomic force spectroscopy

Mark C. Leake [a], Anika Grützner [b], Martina Krüger [b], Wolfgang A. Linke [b,*]

[a] Clarendon Laboratory, University of Oxford, Parks Road, Oxford OX1 3PU, UK
[b] Physiology and Biophysics Unit, University of Muenster, Schlossplatz 5, D-48149 Muenster, Germany

Received 27 November 2005; accepted 20 February 2006
Available online 25 April 2006

Abstract

Titin is a giant protein responsible for passive-tension generation in muscle sarcomeres. Here, we used single-molecule AFM force spectroscopy to investigate the mechanical characteristics of a recombinant construct from the human cardiac-specific N2B-region, which harbors a 572-residue unique sequence flanked by two immunoglobulin (Ig) domains on either side. Force-extension curves of the N2B-construct revealed mean unfolding forces for the Ig-domains similar to those of a recombinant fragment from the distal Ig-region in titin (I91–98). The mean contour length of the N2B-unique sequence was 120 nm, but there was a bimodal distribution centered at ~95 nm (major peak) and 180 nm (minor peak). These values are lower than expected if the N2B-unique sequence were a permanently unfolded entropic spring, but are consistent with the ~100 nm maximum extension of that segment measured in isolated stretched cardiomyofibrils. A contour-length below 200 nm would be reasonable, however, if the N2B-unique sequence were stabilized by a disulphide bridge, as suggested by several disulphide connectivity prediction algorithms. Since the N2B-unique sequence can be phosphorylated by protein kinase A (PKA), which lowers titin-based stiffness, we studied whether addition of PKA (+ATP) affects the mechanical properties of the N2B-construct, but found no changes. The softening effect of PKA on N2B-titin may require specific conditions/factors present inside the cardiomyocytes.

Keywords: Connectin; Titin; Single-molecule; Muscle mechanics; Elasticity; AFM spectroscopy; Protein unfolding; Immunoglobulin domain; Protein kinase A

1. Introduction

The molecular basis for the generation of passive-tension and elasticity in vertebrate striated muscle is well-established to be due primarily to the titin filament system (Opitz et al., 2003; Tskhovrebova and Trinick, 2004; Granzier and Labeit, 2004; Prado et al., 2005). Titins, also known as connectins (Maruyama et al., 1976; Wang et al., 1979), constitute a super-family of large elastic muscle proteins (M_w, 3.0–3.7 MDa) with a highly modular structure. A single titin molecule is in excess of 1 μm in length and is composed of up to 300 domains of the immunoglobulin-like (Ig) or fibronectin-like type, interspersed with unique sequences (Labeit and Kolmerer, 1995). The molecule spans half of a sarcomere, the structural unit of skeletal and cardiac muscle cells, but only the titin segment in the so-called I-band region contributes to muscle elasticity (Fig. 1A) since the remainder is bound firmly to either the thick filament system or the Z-disks (Miller et al., 2004, and references therein).

Single-molecule studies have shown that the elastic properties of titin can be characterized by the sum of several ostensibly independent molecular springs (Li et al., 2002; Leake et al., 2004; Watanabe et al., 2002b). The molecular mechanism of titin elasticity appears to be mainly entropic in nature but an additional component may be due to the unraveling of Ig-domains (Minajeva et al., 2001). Under conditions of high force these domains unfold (Tskhovrebova et al., 1997;

* Corresponding author. Fax: +49 251 8324723.
E-mail address: wlinke@uni-muenster.de (W.A. Linke).

1047-8477/$ - see front matter © 2006 Elsevier Inc. All rights reserved.
doi:10.1016/j.jsb.2006.02.017

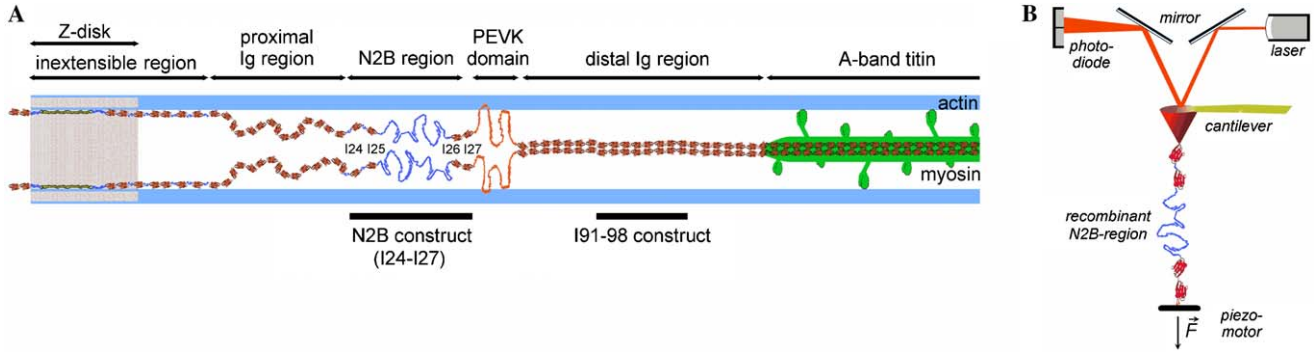

Fig. 1. Atomic force microscope (AFM) force spectroscopy of titin constructs. (A) Schematic of I-band titin domains (N2B-isoform) in the cardiac sarcomere (modified after Neagoe et al. (2003)). Shown are the positions of the recombinant N2B (I24–27) and I91–98 constructs stretched by AFM. (B) Schematic of the AFM setup.

Kellermayer et al., 1997; Rief et al., 1997) and in doing so may act as shock-absorbers to minimize damage to the delicate muscle architecture and allow titin to continue a role for passive-tension generation during pathophysiological stretch (Agarkova and Perriard, 2005). Ig-domain unfolding could also contribute to the viscoelastic properties of muscle (Minajeva et al., 2001; Linke and Fernandez, 2002; Linke and Leake, 2004). Both single-molecule investigations (Rief et al., 1998; Li et al., 2002; Watanabe et al., 2002a) and bulk chemical-denaturation studies (Politou et al., 1995) have suggested that the stability of Ig-domains may vary over several orders of magnitude. When titin-like Ig-domains unfold, they also have the potential to refold under substantial forces of up to 30 pN (Bullard et al., 2006).

The so-called N2B-region within I-band titin is a cardiac-specific segment containing a large unique sequence of 572 amino-acid residues bordered by Ig-domains (Fig. 1A). The mechanical characteristics of these Ig-domains (I24–I27) had been unknown before and were studied in the present work. The N2B-unique sequence (N2B-Us) has earlier been shown to extend towards the upper physiological sarcomere length (SL) range, thereby contributing to the passive-tension generation of cardiac myofibrils (Linke et al., 1999; Helmes et al., 1999). Under conditions of cardiac ischemia both the N2B-Us and the I26/27 Ig-domains of the N2B region associate with the chaperone α-B-crystallin (Bullard et al., 2004). Furthermore, the N2B-Us binds DRAL/FHL-2, which targets metabolic enzymes to the I-band of the cardiac sarcomere (Lange et al., 2002). The N2B-Us has been characterized by single-molecule mechanical studies as having different compliance properties to the rest of the elastic regions of the titin molecule (Li et al., 2002; Watanabe et al., 2002b). There is evidence from myocyte studies that the N2B-Us can be phosphorylated by protein kinase A (Yamasaki et al., 2002), which causes a drop in myocardial passive stiffness (van Heerebeek et al., 2006). Whether the PKA effect on N2B can be seen at the single-molecule level in vitro had not yet been determined.

Here, we generated a recombinant fragment containing the entire human N2B region, in which the unique sequence is flanked by two Ig-domains on either side (Fig. 1A). The force-extension relationship of the N2B construct was analyzed by single-molecule AFM force spectroscopy (Fig. 1B) and a possible mechanical effect of PKA-induced phosphorylation was tested. We found that the N2B-Us does not extend to the contour length of >200 nm expected from a permanently unfolded entropic spring of 572 residues. This finding, also corroborated by titin extensibility studies on isolated single cardiomyofibrils, may be explained by the presence of a disulphide bridge within the N2B-Us, which was suggested by disulphide connectivity prediction algorithms. Experimental conditions not matching the environment of titin in muscle cells could be a reason for an observed lack of changes in mechanical properties of the recombinant N2B-construct upon addition of PKA in the presence of ATP.

2. Materials and methods

2.1. Expression and purification of titin construct

A construct spanning two complete Ig-domains either side of the entire human N2B-region (Lange et al., 2002) was sub-cloned into a pGEX vector with a pEGFP-C1 compatible cloning site and inclusive thrombin cleavage site. This construct, I24–27 (Fig. 1), contains the entire human N2B-region plus one additional C-terminal domain, the I27 Ig-domain (formerly called I19 domain) according to the nomenclature by Bang et al. (2001). (Note that we do not use the nomenclature of titin domains after Labeit and Kolmerer (1995), which is often used in single-molecule work!) The pGEX-N2B plasmid was transformed into an *Escherichia coli* expression system generating a GST-N2B fusion of the correct molecular weight (see Fig. 2A). Purification was by a standard Glutathione–Sepharose 4B pull-down assay followed by thrombin cleavage for GST removal. The I91–98 distal Ig-domain construct (Fig. 1A) was kindly donated by Prof. Mathias Gautel (King's College, London).

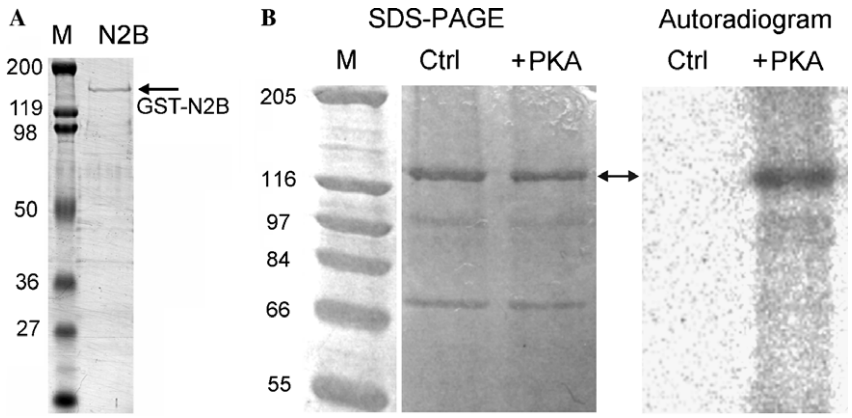

Fig. 2. Expression and phosphorylation of the recombinant N2B-construct (I24–27). (A) SDS–gel electrophoresis of purified GST-N2B product (right lane) compared against molecular weight markers (left lane), values marked in kDa. (B) Autoradiography detects phosphorylation of the N2B-construct by catalytic subunit of protein kinase A (PKA) in the presence of ATP. Ctrl, no PKA added. Lanes were loaded with 2.5 μg (Ctrl) and 1.5 μg (+PKA) protein. M, size marker.

2.2. ^{32}P autoradiography

Phosphorylation of the recombinant N2B-construct was probed by standard autoradiography (Witt et al., 2001). Briefly, the N2B-construct (1.5 or 2.5 μg) was incubated with the catalytic subunit of protein kinase A (BIAFFIN, final concentration 1 U/μl in 50 mM Tris–HCl pH 7.5, 10 mM $MgCl_2$, 0.5 mM ATP, 0.06% NaF) in the presence of [γ-^{32}P]ATP (specific activity, 250 μCi/μM) for 60 min at 30 °C. The protein was then denatured, dissolved, electrophoresed on 10% SDS–polyacrylamide gels, and identified by Coomassie-blue staining. The gel was dried and exposed to an autoradiographic film for 24 h at room temperature. ^{32}P-incorporation was visualized by phosphoimaging (Fujifilm BAS-1800 II).

2.3. AFM force spectroscopy

We used a home-built single-molecule atomic force microscope (AFM) consisting of a commercial detector head (Veeco Instruments, Mannheim, Germany) attached to a piezoelectric positioner with strain gauge sensor (P841, Physik Instrumente, Karlsruhe, Germany), giving a z axis resolution of a few nm over a measurable force range of 10–10,000 pN (Linke et al., 2002; Bullard et al., 2004). Force measurement and the control of the movement of the piezoelectric positioner were achieved by two data acquisition boards (PCI 6052E, PCI 6703, National Instruments) using custom-written software (LabView; National Instruments and Igor, Wavemetrics). The spring constant of each individual cantilever (MSCT-AUHW: sharpened silicon nitride; Veeco Metrology Group, Santa Barbara, CA) was calibrated using the equipartition theorem (typically ~40 pN nm^{-1}). Alternatively, some experiments were performed using the Asylum Research Molecular Force Probe AFM, MFP-3D (Atomic Force F&E GmbH, Mannheim, Germany).

In a given experiment 50 μl of a 2 nM solution of the relevant protein were deposited on a freshly coated gold coverslip (consisting of a 40 nm nickel/chromium base layer and 10 nm gold top surface) for 5 min and rinsed with PBS (100 mM sodium chloride and 50 mM sodium phosphate, pH 7.0). Mechanical stretch experiments on the N2B-construct were performed in the presence or absence of protein kinase A (PKA). For the former the coverslip was then rinsed by 50 μl of a PKA/ATP solution (0.5 μg ml^{-1} PKA, 50 μM ATP in PBS), for the latter PBS alone was used. Since some fraction of the PKA molecules may bind to the gold, we estimated that the effective molar ratio of non-surface-bound PKA to N2B-titin construct may be ~5:1, with an error of at least 20%. Experiments on the I91–98 construct were performed in PBS alone. Following 5 min for equilibration, segments of the proteins were then picked up randomly by adsorption to the AFM cantilever tip by pressing down onto the sample for 1 s at high force (several nN), and stretching for several 100 nm. Surface protein density was optimized to ensure a low probability for tethering to the AFM tip (~1 in 50 attempts) to minimize the chance for capturing two or more molecules and stretching them simultaneously. Such events could be seen as overlapping sawtooth patterns and readily distinguished from the regularly spaced sawtooth pattern that identified a single-molecule. Experiments were performed at a room temperature of 22 °C. The pulling stretch rate for all force-extension traces usually was 1 μm s^{-1}.

2.4. Analysis of force-extension traces

Protein elasticity was modeled using the worm-like chain (WLC) approach of pure-entropic elasticity (Marko and Siggia, 1995)

$$F = \left(\frac{k_B T}{L_p}\right)\left[\frac{1}{4(1-x/L_c)^2} - \frac{1}{4} + \frac{x}{L_c}\right]$$

F is the entropic-based force, L_p is the persistence length, x is end-to-end extension, L_c is contour length of the stretched molecule, k_B is Boltzmann's constant, and T is

absolute temperature. The adjustable parameters were the persistence and the contour lengths. Sawtooth force peaks were detected by an automated custom-written algorithm (LabView), discarding the final force peak in each trace as detachment from the coverslip and/or AFM tip. Continuous inter-peak segments of each force-extension trace were then fitted by a WLC, using a convergence tolerance of 1 nm for L_c and 0.05 nm for L_p. If the difference in L_c for adjacent segments fell within the range 24–32 nm for a given fixed L_p then the force peak of the preceding segment was assigned as an Ig-domain unfolding event (Rief et al., 1997; Li et al., 2002).

2.5. Disulphide connectivity prediction for the human N2B-unique sequence

Disulphide bonds in the N2B-Us were predicted with two different novel algorithms. The DiANNA (DiAminoacid Neural Network Application) web-server (http://clavius.bc.edu/~clotelab/DiANNA/) runs a disulphide connectivity algorithm (version 1.0, January 2005) utilizing a novel architecture neural network. A diresidue Neural Network (Ferre and Clote, 2005) is trained to recognize pairs of bonded half-cysteines given input of half-cysteines symmetric flanking regions. The network-training uses disulphide bond information derived from high-quality protein structures (Vullo and Frasconi, 2004), including evolutionary as well as secondary structure information. A running window PSIPRED is first performed on the whole input sequence to predict the secondary structure (helix, coil, and sheet) followed by PSIBLAST to produce the profile of each position within the running window (Jones, 1999).

The DISULFIND web-server (http://cassandra.dsi.unifi.it/disulfind) employs an SVM binary classifier to predict the bonding state of each cysteine (Ceroni et al., 2003), followed by a refinement stage that collectively classifies all the cysteines in the chain. A bidirectional recurrent neural network (BRNN), similar to DiANNA, and a Viterbi decoder finds the maximum likelihood bonding state assignment which satisfies the constraint for having an even number of disulphide bonded cysteines (ignoring inter-chain bonds).

3. Results

3.1. Expression and phosphorylation of the human N2B-titin construct, I24–27

The full-length N2B-region of human cardiac titin containing the N2B-Us and three Ig-domains, plus the I27-domain (Fig. 1), was expressed in *E. coli* generating a GST-N2B fusion of the correct molecular weight (Fig. 2A). The construct could be readily phosphorylated by the catalytic subunit of PKA in the presence of ATP, as demonstrated by autoradiography (Fig. 2B).

3.2. Mechanical stability of Ig-domains in the human N2B-titin construct, I24–27

Stretching of the N2B-construct resulted in sawtooth force-extension traces (Figs. 3A–C) containing up to four clear force peaks (excluding the final detachment peak). Modeling of the inter-peak force-extension segments suggested most could be characterized by a WLC of

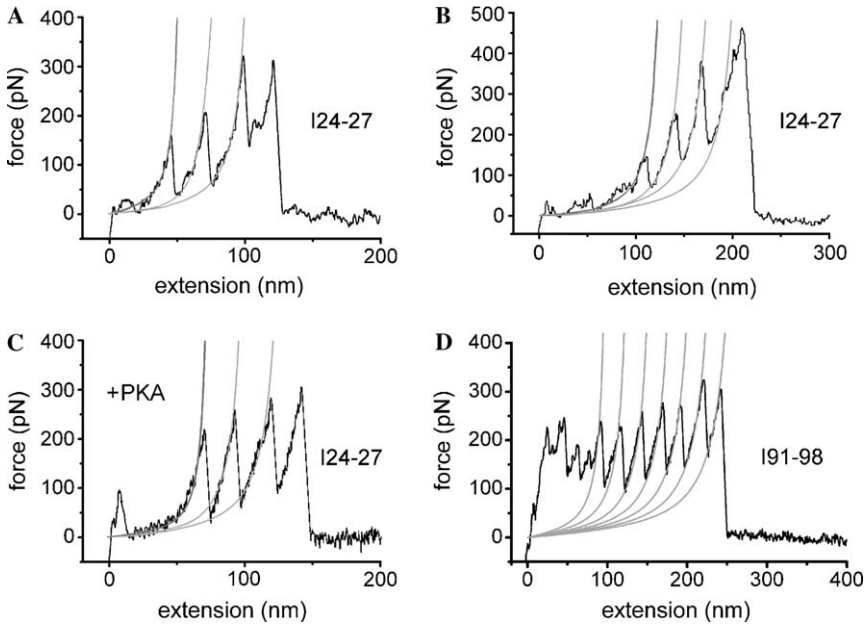

Fig. 3. Force-extension recordings for the recombinant N2B-construct (I24–27), in comparison to an Ig-domain only construct (I91–98). The N2B-construct was stretched in PBS (A) and (B) or in PBS plus PKA in the presence of ATP (C). Unfolding forces were compared to those measured at equivalent stretch rates (1 μm s^{-1}) for the I91–98 construct (D). Grey curves are worm-like chain fits to the sawtooth peaks (dark grey indicates fit to the first force maximum in A–C). The constant contour-length increment between peaks hints at the presence of single-molecule tethers.

persistence length, L_p ~0.2–0.4 nm, with a characteristic spacing in contour length, L_c, between adjacent segments of ~30 nm (Figs. 3A and B).

PKA-dependent phosphorylation of the N2B-region presumably alters titin's mechanical properties (Yamasaki et al., 2002) and though this effect is thought to be mediated by the N2B-Us, we tested whether PKA indeed leaves the Ig-domains of the N2B-segment unaffected. A comparison of sawtooth patterns at equivalent rates of stretch showed no consistent changes in the unfolding force (F_u) of Ig-domains upon addition of PKA in the presence of ATP (Figs. 3A–C). Comparing just the second force peak putatively assigned to unfolding of the same Ig-domain suggested that PKA does not significantly alter the force required to unfold this domain (mean F_u, 220–235 pN; Fig. 4A). Histograms of unfolding forces (all peaks) showed no difference in the mean F_u, in the absence ($F_u = 218 \pm 18$ pN) and presence ($F_u = 228 \pm 15$ pN) of PKA (Figs. 4C and D).

The mechanical properties of the Ig-domains in the N2B-construct were compared to those of a well-studied recombinant Ig-domain construct, I91–98 (elsewhere named I27–34; e.g., Rief et al., 1997; Li et al., 2002), from the distal Ig-domain region (Fig. 1). Stretching this

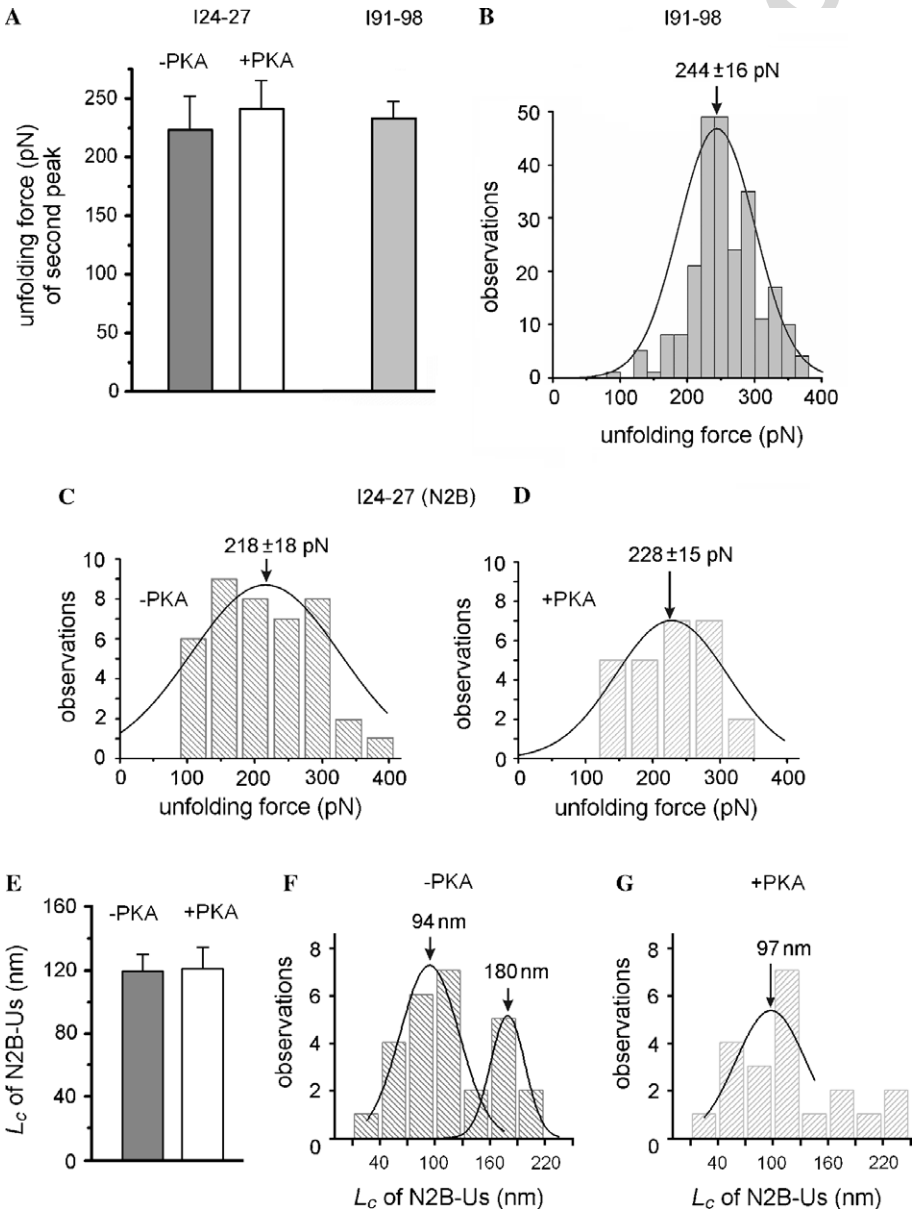

Fig. 4. Mechanical properties of the N2B-region. (A) Ig-domain unfolding forces of the second force peak, collated at a stretch rate of 1 μm s^{-1} for the N2B-construct (I24–27) in the absence and presence of PKA (left two columns), and the I91–98 construct in PBS only (right column). Numbers in each dataset are 14, 11, and 131 (from left to right). Error bars are one SE. (B) Histogram of unfolding forces (all peaks) for the I91–98 construct and Gaussian fit. (C) Unfolding force histogram and Gaussian fit for peaks of N2B-Ig-domains in the absence of PKA. (D) The same, but in the presence of PKA. (E) Mean contour length (L_c) of the N2B-Us calculated from WLC fits of the segment between zero and the first force peak, in the absence ($n = 27$) and presence ($n = 21$) of PKA. Values in (B–E) are mean ± SE. (F) Histogram of contour-lengths values for the N2B-construct in PBS and Gaussian fits showing a major center around 94 nm and a minor center around 180 nm. (G) The same, but for N2B in PKA + ATP.

construct (in PBS) resulted in sawtooth force-extension traces containing between two and seven detected force peaks (Fig. 3D). WLC modeling again suggested that post-Ig-unfold elastic regions of the traces can be characterized by a persistence length, L_p, of ~0.2 nm with a characteristic spacing in contour length, L_c, between adjacent segments of ~28 nm. The Ig-domain unfolding force for just the second force peak at stretch rate 1 μm s^{-1} had a mean value of 230 pN (Fig. 4A) and the mean F_u for all detected force peaks was 244 pN (Fig. 4B).

3.3. Mechanical properties of the N2B-unique sequence with and without PKA

Sawtooth traces of the N2B-construct containing three to four regularly spaced unfolding peaks were analyzed to parameterize the mechanical properties of the N2B-Us (Figs. 3A–C). Modeling the initial trace leading up to the first unfolding peak—presumably corresponding to the stretching of the whole N2B-Us—resulted in WLC fits with L_p between 0.40 and 0.70 nm (in PBS), though the frequent appearance of initial force bumps due to rupture of multimolecular adhesions to the cantilever tip (e.g., Fig. 3B) made the analysis less reliable. Upon addition of PKA the range of persistence length for the initial WLC fit was unchanged at 0.30–0.60 nm.

Datasets measuring the origin-to-first-peak force-extension segment suggested a comparable mean contour length for the N2B-Us of L_c ~120 nm, for stretches in both the presence and absence of PKA (Fig. 4E). Histogram analyses for L_c showed a major peak at ~95 nm under both experimental conditions (Figs. 4F and G). However, there was an additional minor peak centered around 180 nm for N2B-Us stretched in PBS only (Fig. 4F), and a substantial number of long L_c-values up to 240 nm appeared when N2B-Us was stretched in the presence of PKA (Fig. 4G). A predominant contour length of 90–100 nm is lower than what might be expected from sequence data alone, based on a putative random-coil of 572 residues.

3.4. Limited extensibility of the N2B-unique sequence in cardiac myofibrils

To follow up on this point, we compared the L_c of the N2B-Us measured by AFM force spectroscopy with the maximum extension of that titin segment determined by immunostaining methods on myofibrils (Fig. 5). Two different anti-titin antibodies directly flanking the N2B-Us (I25, I26; Fig. 5A) have been used by us previously to stain cardiac sarcomeres at different degrees of stretch (the antibodies were formerly named I17 and I18, respectively; Linke et al., 1999) and to obtain the SL-dependent translational mobility of both antibody epitopes (Figs. 5B and C). Here, we compiled data from Linke et al. (1999) and extended the analysis to the highly stretched SLs to calculate the maximum extension of the full N2B-Us in the sarcomere up to a length of ~2.9 μm (Fig. 5C, inset). At the longer SLs the extension of the N2B-Us leveled out at ~100 nm, suggesting that also in situ this region extends to a contour length lower than expected from a permanently unfolded random-coil.

4. Discussion

Single-molecule AFM force spectroscopy has been used for almost a decade to help establish the mechanical behavior of individual domains of the giant muscle protein titin (e.g., Rief et al., 1997, 1998; Carrion-Vazquez et al., 1999; Li et al., 2002; Watanabe et al., 2002b; Scott et al., 2002). Various I-band titin domains have been analyzed, particularly those from the proximal and distal Ig-domain segments (Fig. 1A), and also the PEVK-domain is mechanically well-studied at the single-molecule level (Li et al., 2001, 2002; Linke et al., 2002; Watanabe et al., 2002b; Leake et al., 2004; Nagy et al., 2005). In contrast, less is known about the cardiac-specific N2B-region (Fig. 1A), of which only the unique sequence was investigated previously by single-molecule AFM (Li et al., 2002; Watanabe et al., 2002b). Here, we cloned a recombinant fragment containing the full N2B-region and used AFM force spectroscopy to measure the mechanical characteristics of the N2B-Us as well as the Ig-domains. Comparing the Ig-domain stabilities of the N2B-region with those of a recombinant fragment of distal Ig-domains (I91–98) at equivalent rates of stretch, we found similar unfolding forces (mean, ~220–240 pN). Further, the N2B-specific Ig-domains showed a rather large range of unfolding forces (100–400 pN) comparable to those found among distal Ig-domains (Rief et al., 1997; Li et al., 2001; Watanabe et al., 2002a). Thus, the Ig-domains of the N2B-region are mechanically similar to other Ig-domains in titin.

The wide interest in the unfolding characteristics of titin Ig-domains notwithstanding, it is still controversial whether or not these domains unfold in muscle sarcomeres (Minajeva et al., 2001; Trombitas et al., 2003; Linke and Leake, 2004). Based on the observation of higher mechanical stability of distal Ig-domains compared to proximal domains (Li et al., 2002), it is likely that the distal Ig-domains do not unfold in situ (Linke et al., 1999; Tskhovrebova and Trinick, 2001; Linke and Fernandez, 2002). The high mean stability of the N2B-specific Ig-domains found here suggests that most of these domains may remain folded during normal cardiac function as well. However, with some Ig-domains in the N2B-region unfolding at forces as low as 100 pN at a stretch rate of 1 μm s^{-1}, it cannot be excluded that a few of these domains do unfold in the sarcomere during high physiological stretch, as suggested earlier for the proximal Ig-domains (Linke et al., 1999; Linke and Fernandez, 2002; Li et al., 2002; Bullard et al., 2004).

Studying the mechanical characteristics of the N2B-Us bordered by the naturally flanking Ig-domains, we collected evidence that this unique sequence may not behave as a

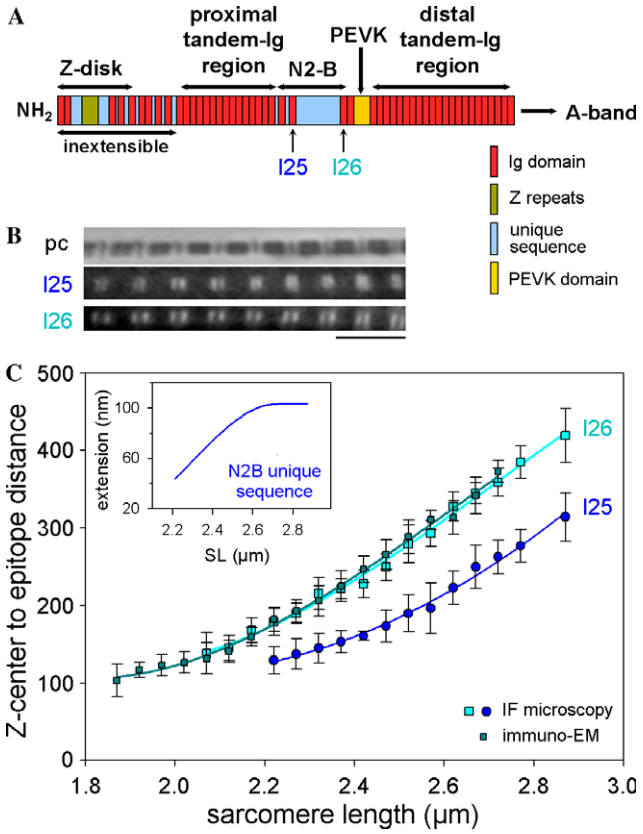

Fig. 5. Extensibility of the N2B-Us in rabbit cardiac myofibrils. (A) Schematic view of the domain architecture of the elastic region of the cardiac N2B-titin isoform (after Labeit and Kolmerer, 1995). Epitope locations of anti-titin antibodies (I25 and I26) flanking the N2B-Us, which were used for immunostaining experiments, are indicated by arrows. (B) Immunofluorescence images of single cardiac myofibrils stretched in relaxing buffer and labeled with the two different antibodies at SL 2.7 μm. pc, Phase image; bar, 5 μm. (C) Distance between *Z* line center and nearest antibody epitope for a large range of SLs, measured by immunofluorescence (IF) and immunoelectron microscopy. Data were compiled from Linke et al. (1999) and some points were added for SL ~2.9 μm. Symbols are means ± SD, fits are three-order regressions. (Inset) Stretch-dependent extension of the N2B-Us in the sarcomere. Note the distinct plateau at SL < 2.6 μm showing a maximum extension of ~100 nm.

permanently unfolded, putative random-coil segment, contrary to previous belief (Li et al., 2002; Watanabe et al., 2002b). The mean contour length of the N2B-Us (120 nm) reached much less than the 220 nm expected from a random-coil of 572 residues. Elsewhere, mean contour-length values above 200 nm were observed in single-molecule AFM studies using the N2B-Us alone (Watanabe et al., 2002b) or the N2B-Us flanked by rows of I91 Ig-domains (Li et al., 2002). In our hands, there was a bimodal distribution of contour-length values with two centers at 90–100 nm (major peak) and ~180 nm (minor peak). In an attempt to explain this unexpected finding, we considered the possibility that there could be some intramolecular structuring within the unique sequence, more specifically an S–S bond between the cysteines (the human N2B-Us has six cysteines; Labeit and Kolmerer, 1995) which the AFM cannot break. Two different web-based algorithms, DiANNA and DISULFIND (see Section 2), were used for disulphide connectivity prediction.

Surprisingly, a high propensity for disulphide bridge formation was suggested by both algorithms, although results differed with regard to the position of the bond (Fig. 6A). DISULFIND predicted connectivity between cysteines in position seven (confidence eight out of nine) and position 100 (confidence four out of nine) in the 572-residue human N2B-Us, whereas DiANNA predicted bonding between cysteines 100 and 445 (probability, 0.961); all other cysteines are unlikely to be bonded (Fig. 6A). An S–S bridge between residues 7 and 100 would suggest that the "free" bit of the N2B-Us stretched has a contour length of ~0.38 nm * 480 = ~180 nm. If the S–S were between residues 100 and 445, the free contour length would be 0.38 nm * 227 = ~90 nm (Fig. 6B). Although, it could just be coincidental, it is remarkable that these contour-lengths values exactly match the mean values of the two populations for L_c found by us.

Why our L_c values differ from those reported in previous studies (Li et al., 2002; Watanabe et al., 2002b) remains unknown at this stage. Possibly, different conditions during protein expression contribute to the disparity and one can also speculate that the differences may be a consequence of us using the whole "native" N2B-region, including the naturally flanking Ig-domains. When we measured the extensibility of the N2B-Us in the natural setting of the cardiac myofibril, this titin segment extended to no more than ~100 nm even under extreme stretch (Fig. 5). Elsewhere, the N2B-Us could be stretched maximally to ~150 nm in the environment of the sarcomere (Trombitas et al., 1999). Perhaps an important methodological difference between our data and those of Trombitas et al. (1999) is that these authors used reducing agent (DTT, 1 mM) in their relaxing buffer, unlike us (cf., Linke et al., 1999). Inside the muscle cells there is a reducing environment due mainly to the presence of glutathione (GSH) (Rutten et al., 2005) and normally the formation of disulphide bridges is unlikely. However, it is possible that the extensibility and spring force of the N2B-Us are modified under conditions that favor the oxidized state—a scenario that has been proposed also for some titin Ig-domains potentially containing an internal disulfide bridge (Mayans et al., 2001). Whether the redox state indeed modifies the mechanical properties of the N2B-Us is testable in future work both at the single-molecule level and in myofibrils.

Of particular interest in this study was the effect of protein kinase A on the mechanical characteristics of the N2B-region. The addition of PKA (in the presence of ATP) to cardiac myocytes has been shown to decrease passive stiffness (Yamasaki et al., 2002; van Heerebeek et al., 2006) and also β-adrenergic stimulation has, via PKA, a softening effect on resting cardiac muscle (Fukuda et al., 2005). These effects have been explained by PKA-aided phosphorylation of titin's N2B-Us (Yamasaki et al., 2002), although no molecular mechanism is currently known to satisfactorily explain how phosphorylation of

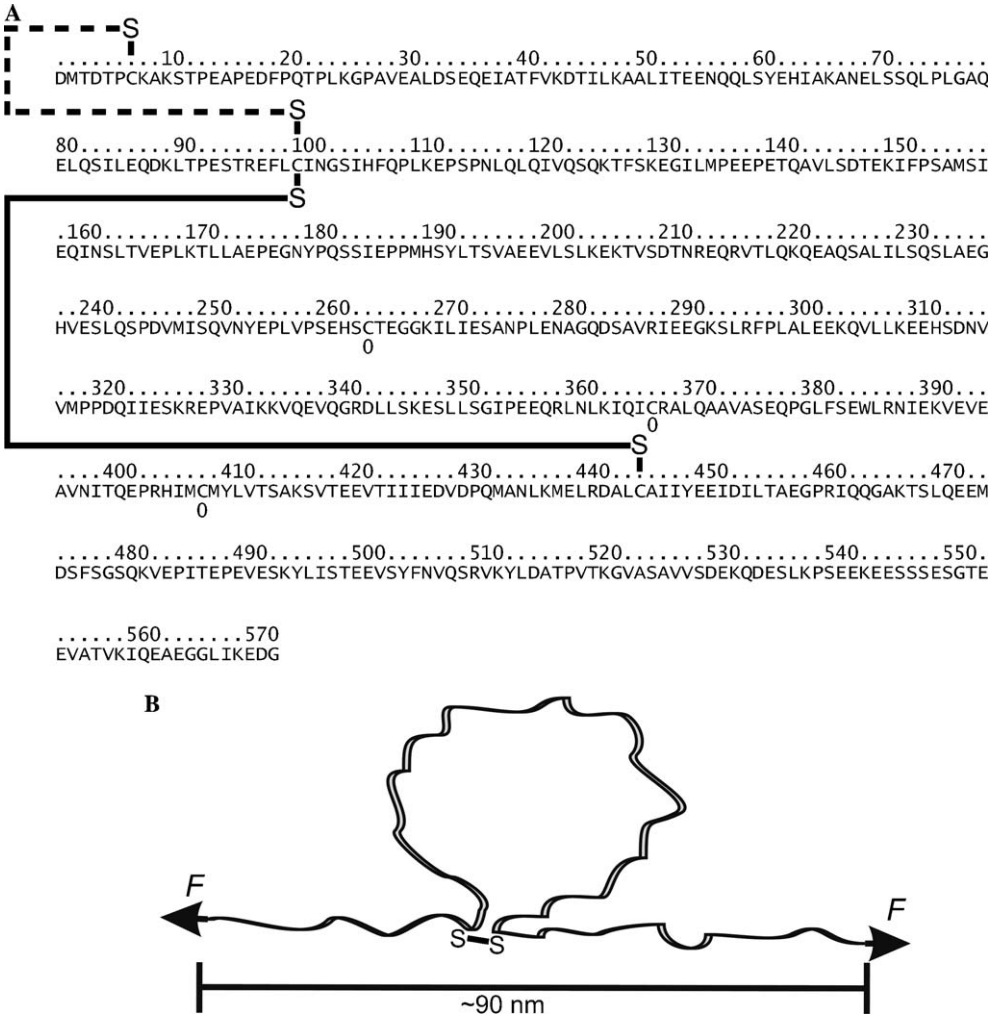

Fig. 6. Disulphide connectivity predictions for the N2B-unique sequence. (A) Sequence of the N2B-Us; residues 1–572 are equivalent to residues 3671–4242 of the human cardiac titin N2B-isoform (Accession No. X90568 in GenBankTM/EBI Data Bank). The output by the DISULFIND (http://cassandra.dsi.unifi.it/disulfind) and DiANNA (http://clavius.bc.edu/~clotelab/DiANNA/) algorithms is shown, suggesting connectivity between cysteines in positions 7 and 100 (dashed line) or in positions 100 and 445 (solid line), respectively. "0" indicates not-bonded cysteine. (B) Schematic of the N2B-Us with a suggested free contour length of ~90 nm if there were a bond between cysteines 100 and 445.

this region could modify titin stiffness. We searched for a direct effect of PKA + ATP on the force-extension behavior of the N2B-titin fragment at the single-molecule level, but found none. Neither the Ig-domain stability nor the contour length/persistence length of the N2B-Us appeared to be affected by PKA. A possible explanation is that PKA + ATP alone is not sufficient to lower N2B stiffness. The kinase, although capable of phosphorylating the N2B-region, might need one or more co-factor(s) to trigger the de-stiffening in cardiac cells. Our results also hint at the possibility that the PKA effect may require reducing conditions. Additional work is needed to establish a molecular mechanism of PKA action on titin.

In summary, we conclude the following about the mechanical properties of titin's N2B-region. (1) The Ig-domains in this region are mechanically similar to other I-band titin domains. (2) The mean contour length of the N2B-unique sequence reached much less than the ~220 nm expected for a fully stretched random-coil of 572 residues, suggesting that this titin segment does not behave as a permanently unfolded entropic spring; the finding might be explainable by the formation of a disulphide bridge under non-reducing conditions. (3) Limited extensibility of the N2B-Us was detected also in isolated, highly stretched, cardiac sarcomeres; possibly then, the N2B spring stiffness is increased under oxidative stress conditions. (4) There was no direct effect of PKA in the presence of ATP on the mechanical characteristics of the recombinant N2B-region, although phosphorylation was detectable.

Acknowledgments

We thank Prof. Julio Fernandez and Dr. Hongbin Li (Columbia University, New York) for advice in developing the AFM force spectroscopy apparatus. We are grateful to Dr. Stephan Lange (King's College London) for donating the original pGEX-DRAL vector for the N2B-construct

and to Dr. Bogos Agianian (EMBL Heidelberg) for the bacterial transformation and final peptide purification. The I91–98 construct was a kind donation of Prof. Mathias Gautel (King's College London). We acknowledge financial support of the Deutsche Forschungsgemeinschaft (SFB 629, TP10 to W.A.L.).

References

Agarkova, I., Perriard, J.C., 2005. The M-band: an elastic web that crosslinks thick filaments in the center of the sarcomere. Trends Cell Biol. 15, 477–485.

Bang, M.L., Centner, T., Fornoff, F., Geach, A.J., Gotthardt, M., McNabb, M., Witt, C.C., Labeit, D., Gregorio, C.C., Granzier, H., Labeit, S., 2001. The complete gene sequence of titin expression of an unusual approximately 700-kDa titin isoform and its interaction with obscurin identify a novel Z-line to I-band linking system. Circ. Res. 89, 1065–1072.

Bullard, B., Benes, V., Garcia, T., Leake, M.C., Linke, W.A., Oberhauser, A.F., 2006. The molecular elasticity of the insect flight muscle proteins projectin and kettin. Proc. Natl. Acad. Sci. USA 103, 4451–4456.

Bullard, B., Ferguson, C., Minajeva, A., Leake, M.C., Gautel, M., Labeit, D., Ding, L., Labeit, S., Horwitz, J., Leonard, K.R., Linke, W.A., 2004. Association of the chaperone alphaB-crystallin with titin in heart muscle. J. Biol. Chem. 279, 7917–7924.

Carrion-Vazquez, M., Oberhauser, A.F., Fowler, S.B., Marszalek, P.E., Broedel, S.E., Clarke, J., Fernandez, J.M., 1999. Mechanical and chemical unfolding of a single protein: a comparison. Proc. Natl. Acad. Sci. USA 96, 3694–3699.

Ceroni, A., Frasconi, P., Passerini, A., Vullo, A., 2003. Predicting the disulfide bonding state of cysteines with combinations of kernel machines. J. VLSI Signal Proc. 35, 287–295.

Ferre, F., Clote, P., 2005. Disulfide connectivity prediction using secondary structure information and diresidue frequencies. Bioinformatics 21, 2336–2346.

Fukuda, N., Wu, Y., Nair, P., Granzier, H.L., 2005. Phosphorylation of titin modulates passive stiffness of cardiac muscle in a titin isoform-dependent manner. J. Gen. Physiol. 125, 257–271.

Granzier, H.L., Labeit, S., 2004. The giant protein titin: a major player in myocardial mechanics, signaling, and disease. Circ. Res. 94, 284–295.

Helmes, M., Trombitas, K., Centner, T., Kellermayer, M., Labeit, S., Linke, W.A., Granzier, H., 1999. Mechanically driven contour-length adjustment in rat cardiac titin's unique N2B sequence: titin is an adjustable spring. Circ. Res. 84, 1339–1352.

Jones, D.T., 1999. Protein secondary structure prediction based on position-specific scoring matrices. J. Mol. Biol. 292, 195–202.

Kellermayer, M.S.Z., Smith, S.B., Granzier, H.L., Bustamante, C., 1997. Folding–unfolding transitions in single titin molecules characterized with laser tweezers. Science 276, 1112–1116.

Labeit, S., Kolmerer, B., 1995. Titins, giant proteins in charge of muscle ultrastructure and elasticity. Science 270, 293–296.

Lange, S., Auerbach, D., McLoughlin, P., Perriard, E., Schafer, B.W., Perriard, J.C., Ehler, E., 2002. Subcellular targeting of metabolic enzymes to titin in heart muscle may be mediated by DRAL/FHL-2. J. Cell Sci. 115, 4925–4936.

Leake, M.C., Wilson, D., Gautel, M., Simmons, R.M., 2004. The elasticity of single titin molecules using a two-bead optical tweezers assay. Biophys. J. 87, 1112–1135.

Li, H., Oberhauser, A.F., Redick, S.D., Carrion-Vazquez, M., Erickson, H.P., Fernandez, J.M., 2001. Multiple conformations of PEVK proteins detected by single-molecule techniques. Proc. Natl. Acad. Sci. USA 98, 10682–10686.

Li, H., Linke, W.A., Oberhauser, A.F., Carrion-Vazquez, M., Kerkvliet, J.G., Lu, H., Marszalek, P.E., Fernandez, J.M., 2002. Reverse engineering of the giant muscle protein titin. Nature 418, 998–1002.

Linke, W.A., Fernandez, J.M., 2002. Cardiac titin: molecular basis of elasticity and cellular contribution to elastic and viscous stiffness components in myocardium. J. Muscle Res. Cell Motil. 23, 483–497.

Linke, W.A., Leake, M.C., 2004. Multiple sources of passive stress relaxation in muscle fibers. Phys. Med. Biol. 49, 3613–3627.

Linke, W.A., Kulke, M., Li, H., Fujita-Becker, S., Neagoe, C., Manstein, D.J., Gautel, M., Fernandez, J.M., 2002. PEVK domain of titin: an entropic spring with actin-binding properties. J. Struct. Biol. 137, 194–205.

Linke, W.A., Rudy, D.E., Centner, T., Gautel, M., Witt, C., Labeit, S., Gregorio, C.C., 1999. I-band titin in cardiac muscle is a three-element molecular spring and is critical for maintaining thin filament structure. J. Cell Biol. 146, 631–644.

Marko, J.F., Siggia, E.D., 1995. Stretching DNA. Macromolecules 28, 8759–8770.

Maruyama, K., Natori, R., Nonomura, Y., 1976. New elastic protein from muscle. Nature 262, 58–60.

Mayans, O., Wuerges, J., Canela, S., Gautel, M., Wilmanns, M., 2001. Structural evidence for a possible role of reversible disulphide bridge formation in the elasticity of the muscle protein titin. Structure (Camb.) 9, 331–340.

Miller, M.K., Granzier, H., Ehler, E., Gregorio, C.C., 2004. The sensitive giant: the role of titin-based stretch sensing complexes in the heart. Trends Cell Biol. 14, 119–126.

Minajeva, A., Kulke, M., Fernandez, J.M., Linke, W.A., 2001. Unfolding of titin domains explains the viscoelastic behavior of skeletal myofibrils. Biophys. J. 80, 1442–1451.

Nagy, A., Grama, L., Huber, T., Bianco, P., Trombitas, K., Granzier, H.L., Kellermayer, M.S., 2005. Hierarchical extensibility in the PEVK domain of skeletal-muscle titin. Biophys. J. 89, 329–336.

Neagoe, C., Opitz, C.A., Makarenko, I., Linke, W.A., 2003. Gigantic variety: expression patterns of titin isoforms in striated muscles and consequences for myofibrillar passive stiffness. J. Muscle Res. Cell Motil. 24, 175–189.

Opitz, C.A., Kulke, M., Leake, M.C., Neagoe, C., Hinssen, H., Hajjar, R.J., Linke, W.A., 2003. Damped elastic recoil of the titin spring in myofibrils of human myocardium. Proc. Natl. Acad. Sci. USA 100, 12688–12693.

Politou, A.S., Thomas, D.J., Pastore, A., 1995. The folding and stability of titin immunoglobulin-like modules, with implications for the mechanism of elasticity. Biophys. J. 69, 2601–2610.

Prado, L., Makarenko, I., Andresen, C., Krüger, M., Opitz, C.A., Linke, W.A., 2005. Isoform diversity of giant proteins in relation to passive and active contractile properties of rabbit skeletal muscles. J. Gen. Physiol. 126, 461–480.

Rief, M., Gautel, M., Oesterhelt, F., Fernandez, J.M., Gaub, H.E., 1997. Reversible unfolding of individual titin immunoglobulin domains by AFM. Science 276, 1109–1112.

Rief, M., Gautel, M., Schemmel, A., Gaub, H.E., 1998. The mechanical stability of immunoglobulin and fibronectin III domains in the muscle protein titin measured by atomic force microscopy. Biophys. J. 75, 3008–3014.

Rutten, E.P., Engelen, M.P., Schols, A.M., Deutz, N.E., 2005. Skeletal muscle glutamate metabolism in health and disease: state of the art. Curr. Opin. Clin. Nutr. Metab. Care 8, 41–51.

Scott, K.A., Steward, A., Fowler, S.B., Clarke, J., 2002. Titin; a multidomain protein that behaves as the sum of its parts. J. Mol. Biol. 315, 819–829.

Trombitas, K., Freiburg, A., Centner, T., Labeit, S., Granzier, H., 1999. Molecular dissection of N2B cardiac titin's extensibility. Biophys. J. 77, 3189–3196.

Trombitas, K., Wu, Y., McNabb, M., Greaser, M., Kellermayer, M.S., Labeit, S., Granzier, H., 2003. Molecular basis of passive stress relaxation in human soleus fibers: assessment of the role of immunoglobulin-like domain unfolding. Biophys. J. 85, 3142–3153.

Tskhovrebova, L., Trinick, J., 2001. Flexibility and extensibility in the titin molecule: analysis of electron microscope data. J. Mol. Biol. 310, 755–771.

Tskhovrebova, L., Trinick, J., 2004. Properties of titin immunoglobulin and fibronectin-3 domains. J. Biol. Chem. 279, 46351–46354.

Tskhovrebova, L., Trinick, J., Sleep, J.A., Simmons, R.M., 1997. Elasticity and unfolding of single molecules of the giant muscle protein titin. Nature 387, 308–312.

van Heerebeek, L., Borbély, A., Niessen, H.W.M., Bronzwaer, J.G.F., van der Velden, J., Stienen, G.J., Linke, W.A., Laarman, G.J., Paulus, W.J., 2006. Myocardial structure and function differ in systolic and diastolic heart failure. Circulation 113, 1966–1973.

Vullo, A., Frasconi, P., 2004. Disulfide connectivity prediction using recursive neural networks and evolutionary information. Bioinformatics 20, 653–659.

Wang, K., McClure, J., Tu, A., 1979. Titin: major myofibrillar component of striated muscle. Proc. Natl. Acad. Sci. USA 76, 3698–3702.

Watanabe, K., Muhle-Goll, C., Kellermayer, M.S., Labeit, S., Granzier, H., 2002a. Different molecular mechanics displayed by titin's constitutively and differentially expressed tandem Ig segments. J. Struct. Biol. 137, 248–258.

Watanabe, K., Nair, P., Labeit, D., Kellermayer, M.S., Greaser, M., Labeit, S., Granzier, H., 2002b. Molecular mechanics of cardiac titin's PEVK and N2B spring elements. J. Biol. Chem. 277, 11549–11558.

Witt, C.C., Gerull, B., Davies, M.J., Centner, T., Linke, W.A., Thierfelder, L., 2001. Hypercontractile properties of cardiac muscle fibers in a knock-in mouse model of cardiac myosin-binding protein-C. J. Biol. Chem. 276, 5353–5359.

Yamasaki, R., Wu, Y., McNabb, M., Greaser, M., Labeit, S., Granzier, H., 2002. Protein kinase A phosphorylates titin's cardiac-specific N2B domain and reduces passive tension in rat cardiac myocytes. Circ. Res. 90, 1181–1188.